

Supporting Information

Visible-light-driven hydrogen evolution from waste toner powder activated by Ni species

Wenyan Zhang^{*a}, Hangmin Guan^{*a}, Yingfei Hu^a, Wei Wang^a, Linyun Hao^{*a}, Xiaoli Yang^a, Wenjie Tian^a

a.College of Material Engineering, Jinling Institute of technology, Nanjing 211169, China

S1. Effect of Cobalt on regulating the activity of waste toner powder

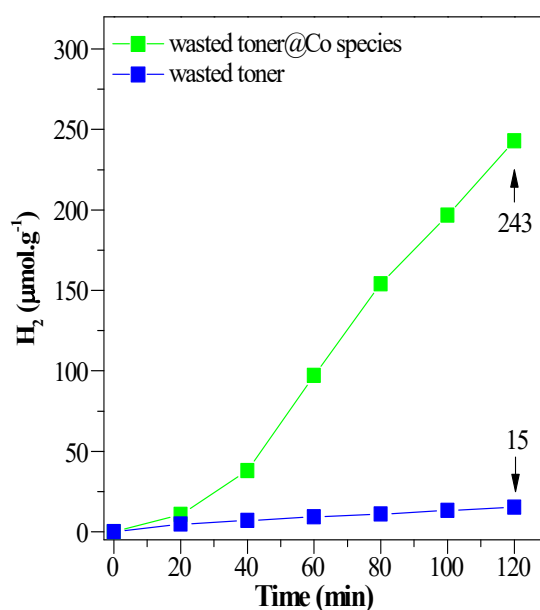


Fig. S1 Hydrogen production as a function of time for pristine waste toner and waste toner activated by Co species (waste toner@Co-species) driven by visible light irradiation ($\lambda \geq 420$ nm), conducted at room temperature in a system with Eosin Y (EY) concentration of 1.0×10^{-3} M in 100 mL 10% (v/v) triethanolamine (TEOA) aqueous solution

We investigated the effect of Cobalt on regulating the activity of waste toner powder in dye-sensitized system. Waste toner@Co-species was prepared through the same method (in-situ photo-reduction) for preparing waste toner@Ni-species. As shown in Fig. S1, H₂ evolution rate of waste toner@Co-species was 243 $\mu\text{mol}\cdot\text{g}^{-1}$ in 2 h, which was about 16 folds of H₂ evolution over pristine waste toner (15 $\mu\text{mol}\cdot\text{g}^{-1}$ in 2 h). Thereby, Co species have similar effect to that of Ni species on activating waste toner for hydrogen evolution, while photocatalytic activity improvement associated with Co species was not as remarkable as that

associated with Ni species. In other words, Ni species are more preferred to enhance the activity of waste toner in our system than Co species.

S2. FTIR characterization of waste toner@Ni-species

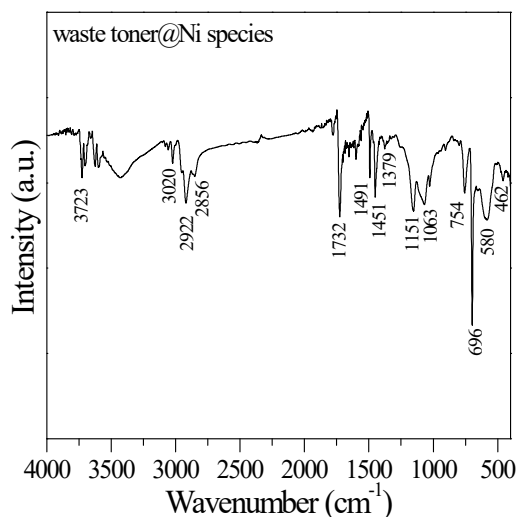


Fig. S2 FTIR spectra of waste toner@Ni-species

[Fig. S2](#) shows FTIR spectrum of waste toner@Ni-species. In [Fig. S2](#), the infrared vibration bands around 1732 cm⁻¹, 1451 cm⁻¹ and 1379 cm⁻¹ correspond to the stretching vibration of COO⁻ group [\[S1\]](#), which indicates that waste toner@Ni-species was dispersed in aqueous system with the aids of hydrophilic COO⁻ group attached to the surface of waste toner@Ni-species. Meanwhile, in [Fig. S2](#), the infrared vibration band around 2922 cm⁻¹ and 2856 cm⁻¹ are attributed to the stretching vibration of -CH group from organic compound in waste toner. The band around 696 cm⁻¹ is assigned to out of plane bending of -CH group. Additionally, the vibration band around 521 cm⁻¹ and 462 cm⁻¹ are assigned to the Fe-O bonds of iron oxide in waste toner [\[S2\]](#).

S3. BET analysis of waste toner powder and waste toner@Ni-species

[Fig. S3 \(a\)](#) shows N₂ adsorption–desorption isotherms of waste toner powder. [Fig. S3 \(a\)](#) indicates there was almost no pore in pristine waste toner powder. N₂ adsorption–desorption isotherms of waste toner@Ni-species is presented in [Fig. S3 \(b\)](#), which indicates the

formation of small amount of pores on pristine waste toner due to the deposition of Ni species. Specific surface area of pristine waste toner powder and waste toner@Ni-species was obtained from BET analysis, which was about 0.0168 m²/g for pristine waste toner and 0.1337 m²/g for waste toner@Ni-species. Namely, specific surface area of waste toner was increased by 7 times due to the deposition of Ni species.

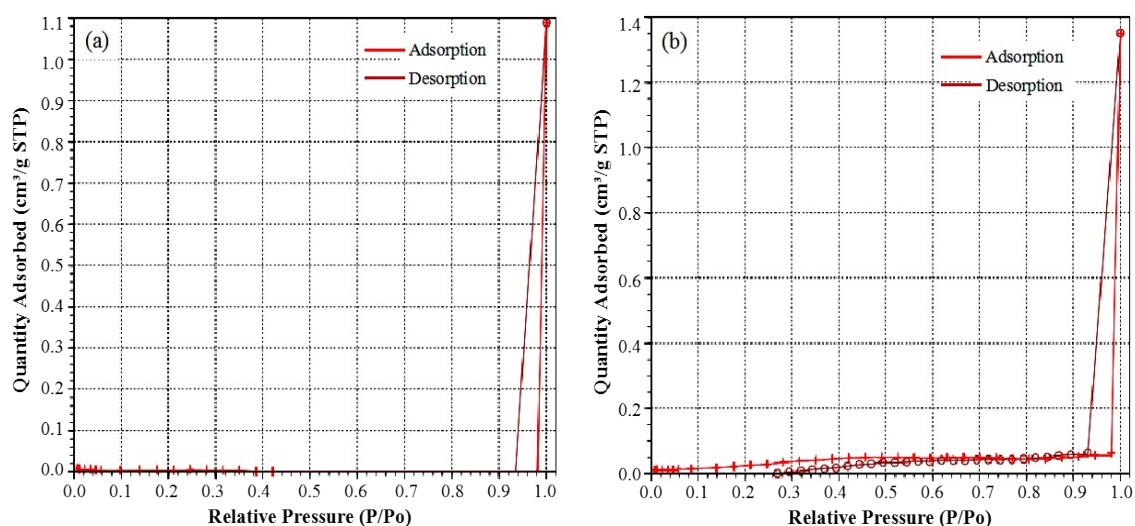


Fig. S3 Nitrogen adsorption-desorption isotherms of (a) waste toner and (b) waste toner@Ni-species

S4. UV-Vis absorption of pristine waste toner

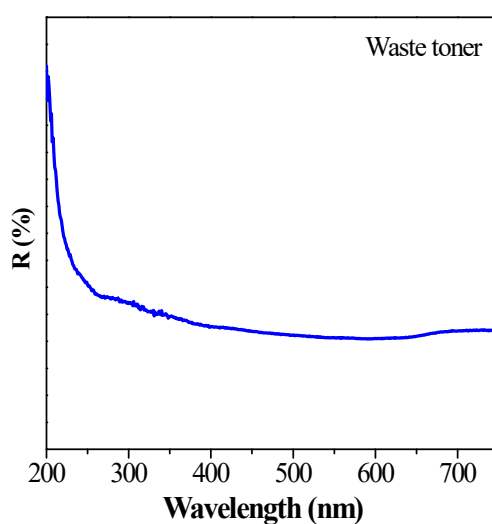


Fig. S4 UV-Vis DRS spectrum of pristine waste toner

We recorded UV-Vis DRS spectrum of pristine waste toner powder. As shown in [Fig. S4](#), pristine waste toner did not exhibit obvious visible light harvesting performance. Thus, light

harvesting capability of the reaction system is mainly assigned to the absorption of EY dye, given UV-Vis spectrum of EY and AQE of waste toner@Ni-species (see Fig. 1(b1,c1)).

S5. Morphology and size distribution of Ni species on waste toner

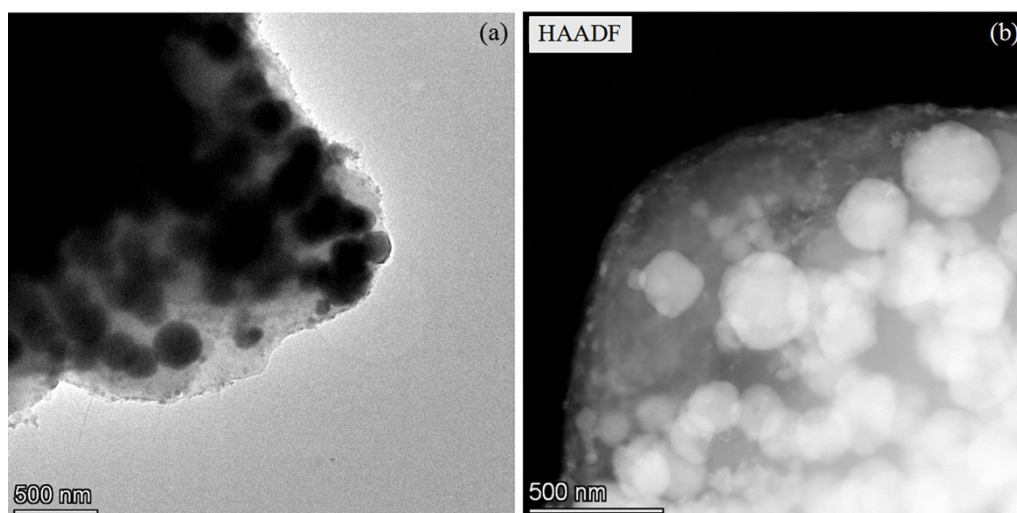


Fig. S5 (a) HRTEM image of waste toner@Ni-species (b) HAADF-STEM (high angle annular dark field scanning transmission electron microscopy) image of waste toner@Ni-species

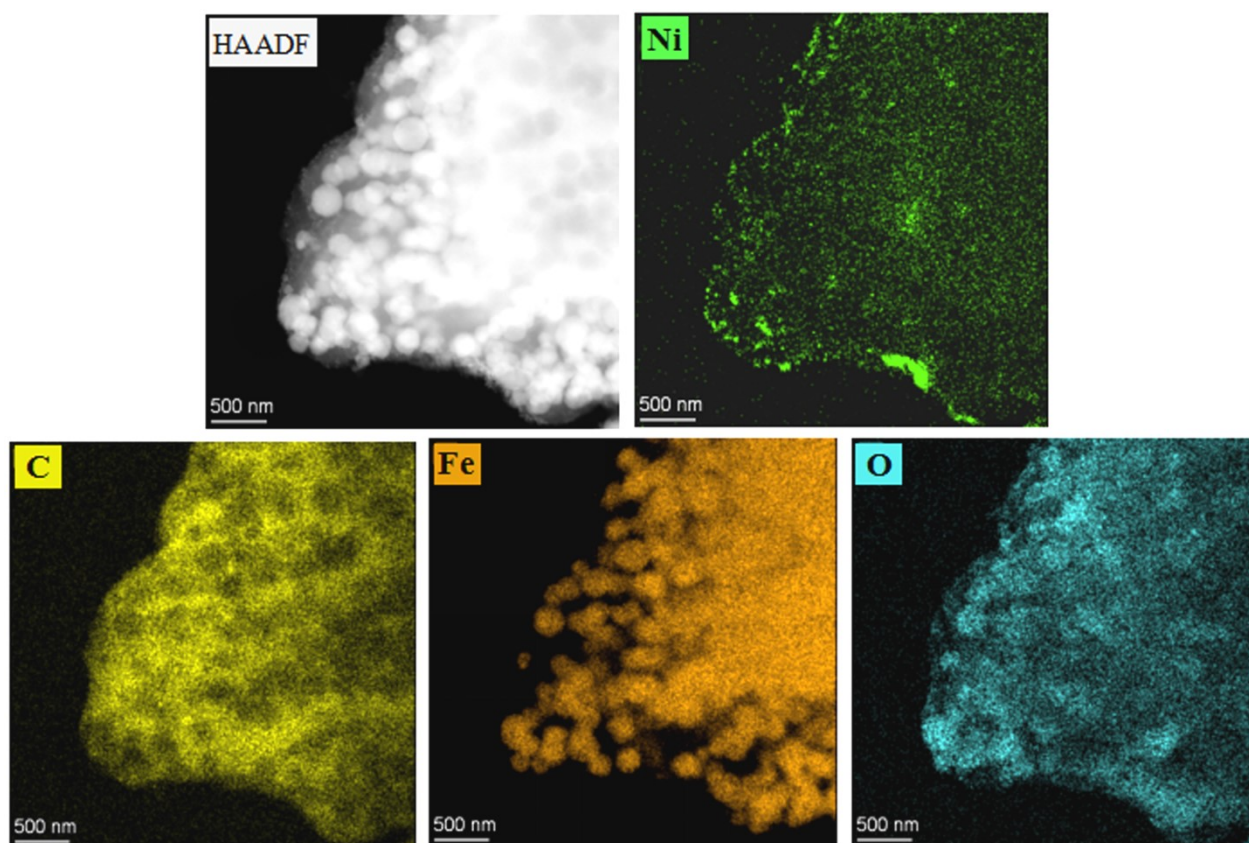


Fig. S6 HAADF-STEM (high angle annular dark field scanning transmission electron microscopy) image

and elemental mapping images of waste toner@Ni-species

Here, we investigated Ni species on waste toner further through the characterization of TEM and HAADF-STEM (high angle annular dark field scanning transmission electron microscopy), which provided more details and information for Ni species. Fig. S5 (a) shows TEM image of waste toner@Ni-species. It can be observed from Fig. S5 (a) that there are black “balls” encapsulate in gray layer. These black “balls” are iron oxide, and the gray layer is carbon layer (the color of carbon layer was much lighter than iron oxide due to contrast). It is noted that in Fig. S5 (a), there are many nano scaled particles assembled on the surface of carbon layer. Fig. S5 (b) presents HAADF-STEM image of waste toner@Ni. In consistent with Fig. S5 (a), there are many white “balls” (iron oxide) enclosed in carbon layer in Fig. S5 (b). Moreover, Fig. S5 (b) clearly shows the existence of many nano scaled particles on carbon layer of waste toner. To investigate the composition of these nano scaled particles, we recorded HAADF-STEM image together with elemental mapping images for waste toner@Ni-species (as shown Fig. S6). It is known from Fig. S6 that these small particles distributed on the surface of carbon layer should be Ni species.

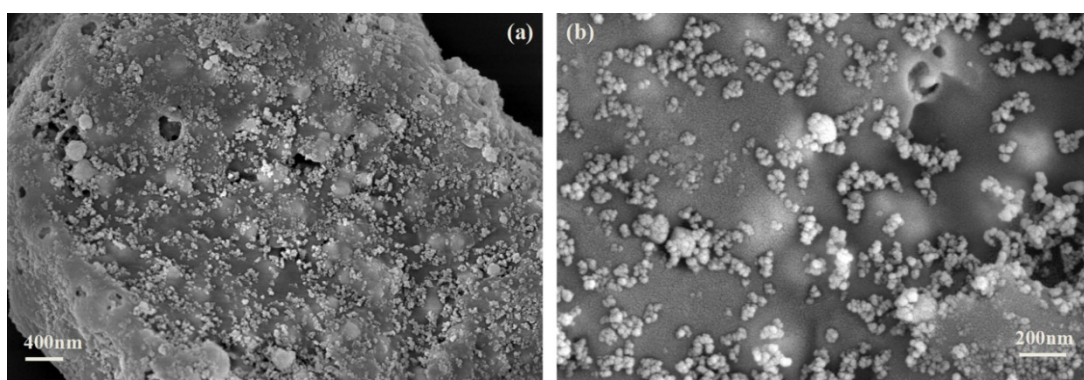


Fig. S7 (a) FESEM image of the surface of waste toner@Ni-species; (b) Magnification of Fig. S7 (a)

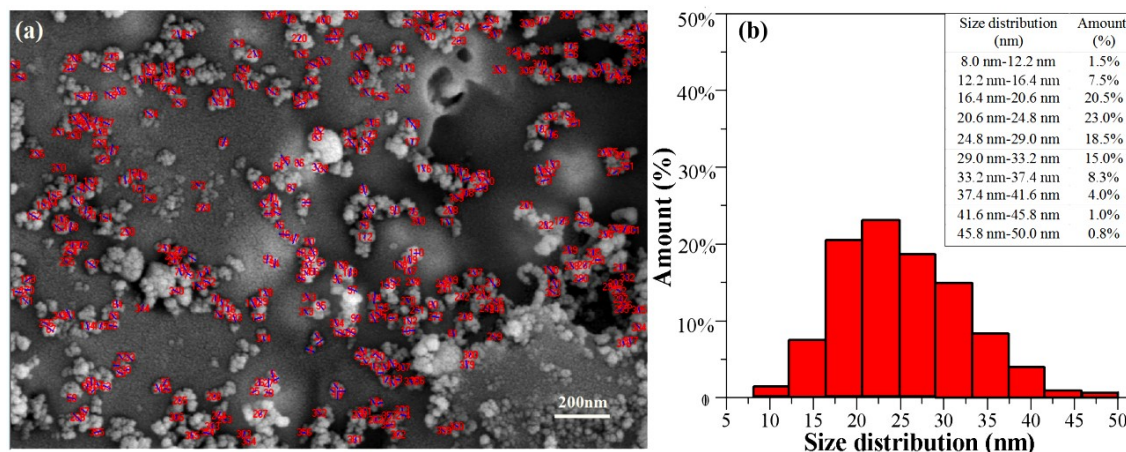


Fig. S8 (a) Marks of 400 particles selected from Fig. S7 (b); (b) Size distribution of particles deposited on toner

Here, we tried and found it was not feasible to get good HRTEM image for studying the particle size of Ni species. As waste toner was relatively big, with the size of several micrometer (as shown in Fig. 3), it was difficult for incident electrons to transmit waste toner to form clear HRTEM image. Thus, we have to resort to FESEM characterization to investigate particle size distribution of Ni species on toner (see Fig. S7, Fig. S8).

Fig. S7 (a) shows FESEM image of the surface of waste toner@Ni-species. Fig. S7 (b) is a magnification image of Fig. S7 (a). As shown in Fig. S7 (a,b), there are many nano scaled particles deposited on the surface of toner. These small particles have irregular morphology, and some particles aggregated with others. We selected 400 particles from Fig. S7 (b) and calculated particle size distribution of them. In order to make the calculation of particle size distribution more accurate, the particles were selected casually and we did not choose those particles which aggregated heavily with other particles. The selected 400 particles are marked, as shown in Fig. S8 (a). Fig. S8 (b) presents size distribution of the selected 400 particles, which shows that most of the particles are distributed in the size of 16 nm ~ 33nm.

Thirdly, we investigated the content of Ni species on the surface of waste toner through EDS characterization. In order to make the results more accurate, we casually selected three small region from waste toner@Ni-species and recorded EDS spectra of the three small region. EDS spectra collected from the three small region are shown in Fig. S9. Elemental contents of the three small region are summarized in Tab. S1. As shown in Fig. S9 and Tab. S1, the content of Ni on the surface of waste toner was about 0.1%.

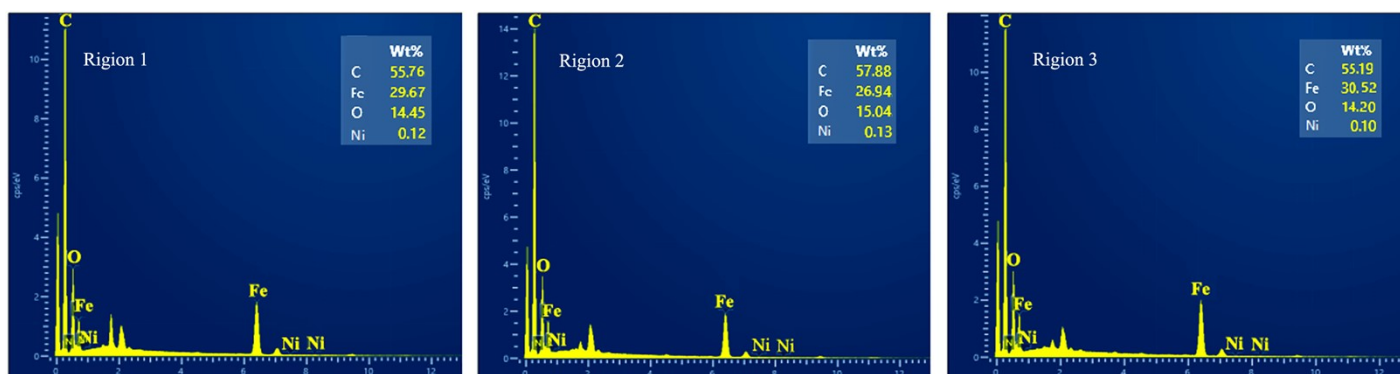


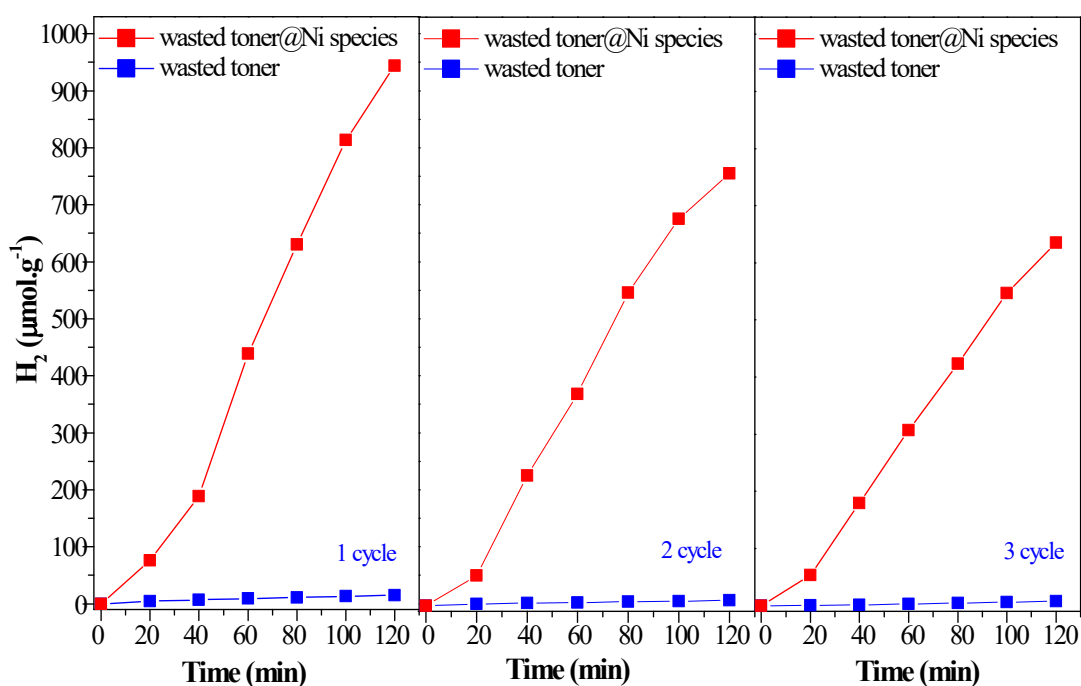
Fig. S9 EDS spectra of casually selected three three small region on waste toner@Ni-species

Tab. S1 Element content of casually selected three three small region on waste toner@Ni-species

| Element | Wt% (Region 1) | Wt% (Region 2) | Wt% (Region 3) |
|---------|----------------|----------------|----------------|
| C | 55.76 | 57.88 | 55.19 |
| Fe | 29.67 | 26.94 | 30.52 |
| O | 14.45 | 15.04 | 14.20 |
| Ni | 0.12 | 0.13 | 0.10 |

S6. Recycle HER experiment over the samples

In this work, we evaluated the catalyst stability of waste toner@Ni-species by repeated cycles. Fig. S10 shows three cycles of hydrogen evolution over waste toner@Ni-species. The H₂ evolution remained about 67% after three cycles. The degradation of catalytic activity during repeated cycles could be related to two causes. One cause is the consumption of sacrificial donor. In the reaction system, tri-ethanolamine (TEOA) played a role as sacrificial donor. The consumption of TEOA could slow down the electron transfer rate between EY and catalyst, as a result declining H₂ evolution rate over photocatalysts. The other cause is related to potential damage of waste toner@Ni-species, which could be induced due to catalysts poisoning during the reaction, the breaking of waste toner powders, as well as the leaching of Ni species from the surface of waste toner.

**Fig. S10** Comparison of HER over waste toner powder and waste toner@Ni-species (Three cycles)

On the other hand, we checked and clarified that NiO particles have lower activity than waste toner@Ni-species in our reaction system for facilitating hydrogen production. Here, we dispersed NiO particles in our reaction system (without waste toner or waste toner@Ni species), and recorded the hydrogen evolution with NiO as catalyst. As shown in Fig. S11, hydrogen evolution over NiO was obviously smaller than that over waste toner@Ni-species. Given this result, it is known that even if NiO leached out from the surface of waste toner and worked in homogeneous phase, they have little contribution to improving hydrogen evolution performance of the system. Meanwhile, this result indicates synergistic interaction occurred between Ni species and waste toner and such interaction was beneficial for improving hydrogen production.

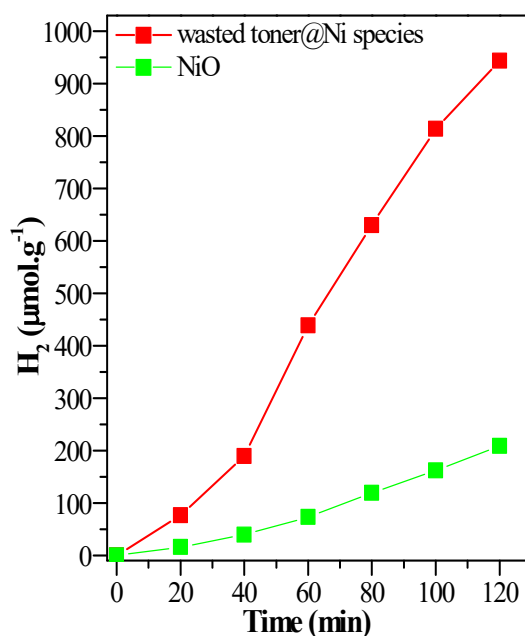


Fig. S11 Comparison of HER over waste toner@Ni-species and NiO

Reference

[S1] R. A. Soomro, A. Nafady, Sirajuddin, N.a Memon, T. H. Sherazi, N. H. Kalwar, *Talanta* 2014, 130, 415–422.

[S2] R. X. Mo, D. Q. Han, C. W. Yang, J. Y. Tang, F. Wang, C. L. Li, *Sensors and Actuators B: Chemical* 2021, 330, 129326.